An investigation of turbulent developing flow at the entrance to a smooth pipe

L. A. Salami*

An attempt is made to explain the flow regimes at the entry region of a pipe. Developing turbulent flow was examined and three theoretical models were evolved to explain the three most important regimes: the region of flat plate flow, the region of transition from flat plate to pipe flow, and the region of boundary layer interaction. The model for the flat plate flow was based on the velocity power law but experimental data showed that the exponent was not constant as generally assumed. There was good agreement between the theoretical models and the experimental data for the boundary layer development.

A simple empirical formula was obtained from which it is possible to predict the length of the entry region. The onset of the increase in turbulence intensity at the core, which marks the start of transition from flat plate flow to pipe flow, seems to occur at a particular Reynolds number, based on distance into the pipe, of about 3.15×10^6. This figure may vary with inlet flow condition.

Introduction

Development of flow at the entry of a pipe has been of interest to many researchers. For instance, because the efficiency of a diffuser is affected by the inlet conditions, researchers in this area have carried out extensive investigations of this type of flow[1-4]. A review of their work is given in Klein[5].

Wang and Tullis[6] also did some work on developing flows before starting an investigation on drag reduction using polymers.

Other researchers wanted to use information on developing flows in their investigations of the effect of upstream velocity profile on meter performance[7,8]. The work described in Ref 7 was carried out at a particular flowrate, and it was noted that there was redistribution of flow after the boundary layer first reached the pipe axis. Because there were some aspects of the work which were still not clearly understood investigation was carried out by Salami[8] at three flowrates. The findings of Jepson and Bean[7] were confirmed for these flowrates, and it was also confirmed that the results obtained were at variance with the conclusions of Fillipov[9], one of the earliest theoretical works on the subject.

The topic is also of importance because it aids the understanding and design of pipe systems, heat exchangers, wind tunnels, etc.

The object of this investigation was to throw more light on the mechanics of turbulent developing flow in a circular pipe. From this understanding a theoretical model is evolved which is used to correlate most of the experimental data obtained, including two regimes of the flow which have, hitherto, not been tackled.

* Faculty of Engineering, University of Benin, Benin City, Nigeria

Literature survey

Publications, mainly in the last two decades, such as Weir *et al*[1], Miller[2], Barbin and Jones[3], Patel[4], and Wang and Tullis[6] have confirmed that the conclusions of earlier researchers such as Fillipov[9] and Ross and Whippany[10], which were mainly theoretical, were at variance with experimental results. Instead of the four regimes assumed in Refs 9 and 10, ie laminar, transitional and turbulent developing flow and fully developed turbulent flow regimes, the former references have demonstrated that there are six regimes. The first of these is laminar and occurs a few diameters into the test length. For higher flowrates there is the transition regime followed by the turbulent developing regime with a central core of low turbulence. In the fourth regime the boundary layer was not only turbulent and developing but in the central core of uniform velocity the turbulence intensity increases very rapidly. Eventually, the boundary layer reaches the pipe axis and marks the beginning of the fifth regime where further mixing continues. This smooths the velocity profile.

The general approach in obtaining a theoretical model for developing flow is to apply the continuity and the momentum integral equations to the flow. From this, and by making suitable assumptions, the rate of increase of momentum thickness θ is obtained in terms of the wall shear stress coefficient. After expressing this in terms of the Reynolds number based on the pipe diameter, the momentum thickness is obtained by integration.

Most models differ mainly in the assumptions made for the velocity distribution. Holdhusen[11], Diessler[12], Fillipov[9], Barbin and Jones[3], and Wang and Tullis[6] assumed the universal semi-log-law while Latzco[13] and Bowles and Brighton[14] assumed $\frac{1}{7}$th power law. Ross and Whippany[10] did not assume any velocity

profile in particular. Most of the models are limited to the first few pipe diameters of the flow. Few have attempted to give a complete correlation for the developing flow region, and then only for laminar flow, such as Mohanty and Asthana[15].

On the experimental side, not many of those who proposed a theory tried to verify them experimentally. Many of those who carried out experimental investigations on developing flow did so with a view to applying the results for other purposes such as those mentioned in the introduction, and they did not bother to evolve a theoretical model for their work. Klein[5] also reviewed some such examples. From this last work it is clear that the results for developing flow partly depend on the upstream flow condition and the geometry of the entrance to the pipe. Thus, sometimes the work done at roughly the same Reynolds number on two different test rigs gave different results.

Some researchers such as Weir *et al*[1], Miller[2], Barbin and Jones[3] and Sale[16], have measured the centreline turbulence. It was found to be low at first, even though the boundary layer was turbulent, but after some distance the turbulence increased rapidly to an almost constant value even before the boundary layer first reached the pipe line axis. Another important finding was the distinction, expressed in terms of distance in pipe diameters, between the point when the boundary layer first reaches the pipe axis and that when the flow is fully developed. These are distinct since it is now recognized that the velocity distribution continues to change long after the boundary layer has reached the pipe axis. In Ref 15 for laminar flow, there is a difference by a factor of four between the two distances, which is quite considerable.

Test rig and experimental procedure

Fig 1 shows the details of the constant-head rig on which the investigations were carried out. A 254 mm diameter pipe from a constant-head tank delivers water to the horizontal Perspex test length, which is 50.8 mm in diameter and 5 m long. The details of the reducing piece, RP, which joins the two pipes together are shown in the insert. The flowrate is obtained by a collect-and-weigh system with a weighing tank capacity of about 5 tonnes.

A pitot wall static combination was used to carry out the traverse of the flow, the pitot tube being actuated by a micrometer arrangement. The outer diameter of the pitot tube was 1.5 mm, the inner 1.0 mm, while the stem was 3.0 mm to make the tube more rigid. As the pitot tube reading is not affected by the stem, the length of the pitot tube at right angles to the stem was made as small as convenient: about 25 mm. Both round and flattened pitot tubes were used although not much difference was noticed in their results. This could be due to the fact that even at the lowest flow rate the Reynolds number of 700 based on the smaller inner tube dimension in the case of a flattened tube, was in the region where error due to viscosity was negligible[17].

Altogether, three flowrates were used. Pressure differences were measured using a Betz water micromanometer for the lowest flowrate when the difference was very small, but ordinary water manometers were used for the medium and the highest flowrates.

Pitot traversing was carried out up to 15D from the end of the test length for each flowrate, where D is the test length diameter. The distance between the sections where traversing took place was small at first, usually 3D, but the interval was increased to 12D towards the end of the test length. Traversing usually started from the pipe axis, and the point where the reading just begins to fall was taken as the edge of the boundary layer. It was generally preferred to traverse the boundary layer along the diameter away from the position where the pitot tube was mounted because it was easier to locate the exact position of the end of the pitot tube as a resistance was experienced when the wall was reached. If traversing took place in the opposite direction it became difficult to know when the tip of the pitot tube had reached the inner wall next to where it was mounted and any undue force tended to straighten the bend.

Most readings of the boundary edge were checked by taking one reading for each direction of traverse along two diameters at right angles except where the boundary layer was so thin that the bend became a problem as already mentioned. Results of boundary layer traverse were the average of the four readings taken at the ends of the two diameters. Wherever possible, at least ten pitot tube pressure readings were taken within the boundary layer. From these results it was possible to confirm that the flow was fairly symmetrical.

During the course of the programme two traversing gears were used. The Perspex one with elongated bolt holes on the flanges enabled the pitot stem to be rotated about the pipe axis by up to 90° and this was

Notation

B	Blockage factor, $1-\frac{U_0}{U_c}$
C_f	Local coefficient of friction
D	Test pipeline diameter
n	Reciprocal exponent in velocity power law $\frac{U}{U_c}=\left(\frac{y}{\delta}\right)^{1/n}$ or $\frac{U}{U_c}=\left(\frac{y}{R}\right)^{1/n}$
R	Pipe radius, $D/2$
Re, Re_x	Reynolds number based on pipe diameter, $U_0 d/\nu$, and on distance into test pipeline from upstream end, $U_0 x/\nu$, respectively
U	Axial velocity at any point at distance y from the pipe wall
U_c	Uniform velocity at the central core
U_0	Mean velocity in the pipe
x	Distance from the start of the test pipeline
δ	Boundary layer thickness
δ^*	Boundary layer displacement thickness
$\Delta\delta$	Change in the boundary layer thickness, $\delta-\delta_3$
θ	Momentum thickness of boundary layer
ν	Kinematic viscosity

Subscripts

1, 2, 3, 4, 5 Flow regime

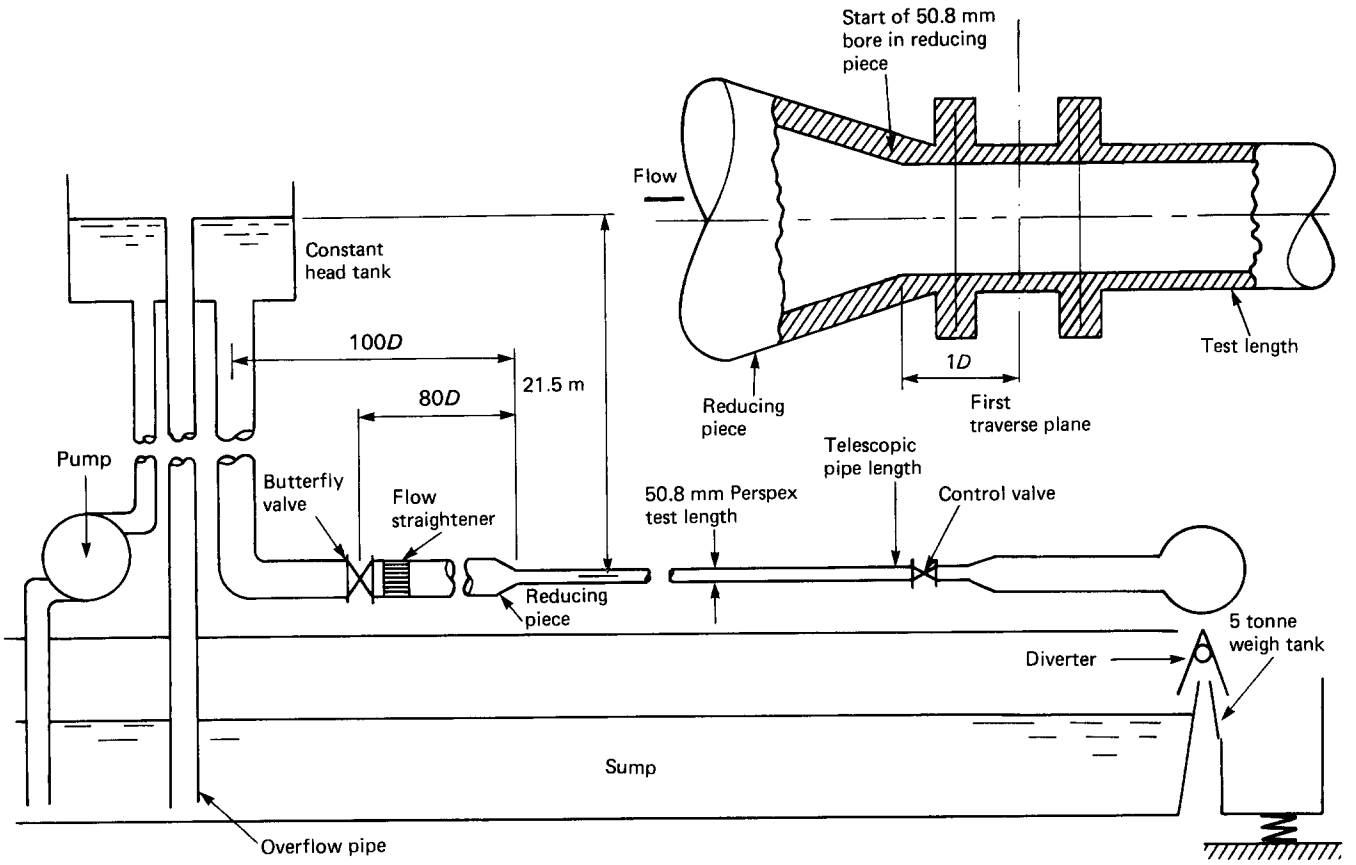

Fig 1 Layout of the constant-head calibration rig. Insert shows details of entry section of pipe

used for the work described above. The other, which could rotate 360° about the pipe axis, was developed mainly to tackle swirling flow measurement. During the commissioning tests, it was used to traverse the flow at a few sections and the results were generally in good agreement with those obtained from the Perspex traversing gear. In fact, it was on the basis of this agreement that the traversing gear was eventually used to investigate swirling flows[18].

The procedure described above took a few weeks to complete. Readings at a few sections were consequently repeated to ensure the former results were repeatable. Agreement was generally fair, this being due perhaps to the temperature being fairly constant throughout the investigation.

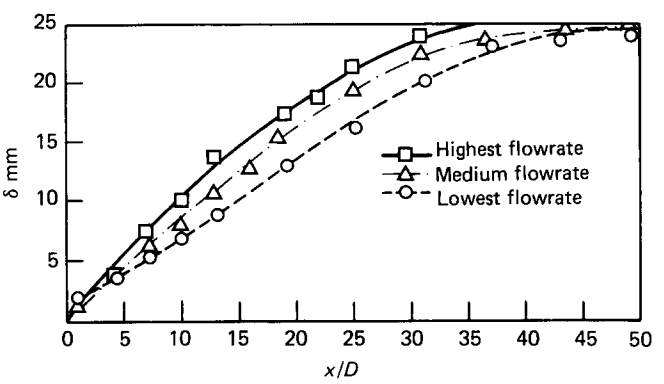

Fig 2 Development of boundary layer in entry portion of pipe for the three selected values of flowrate. Note that the boundary layer reaches the pipe centre at a shorter distance from the reducing piece for the highest flowrate

Experimental results

Fig 2 shows the development of the boundary layer thickness, δ, up to the pipe axis for the three flowrates. The flow at the beginning of the test length, especially for the medium and highest flow, was almost completely uniform ($\delta = 0$). Fig 3 shows the plot of $\log U/U_c$ against $\log y/\delta$ for the three flowrates, where U is the velocity at any point at distance y from the pipe wall, and U_c the velocity at the central core.

From the latter figure it is clear that the velocity profile for the highest and medium flowrates definitely obeys the velocity power law, $U/U_c = (y/\delta)^{1/n}$. With this fact established and the knowledge of the core velocity ratio U_0/U_c, where U^0 is the average velocity, and the boundary layer thickness at any section, it was possible to calculate n using the continuity equation as shown below. The variations of n with distance into the pipe, x/D, were thus obtained for the two flowrates and are shown in Fig 4, where x is the distance in metres into the test length. For the lowest flowrate, the power law did not satisfactorily define its velocity profile except when the boundary layer thickness was almost equal to the pipe radius (Fig 3). The early part of the curve for this flowrate in Fig 4, which corresponds to this portion, is shown in broken lines because it has been obtained as for other flowrates assuming that the velocity profile obeyed the power law.

Fig 4 shows that the value of n dropped

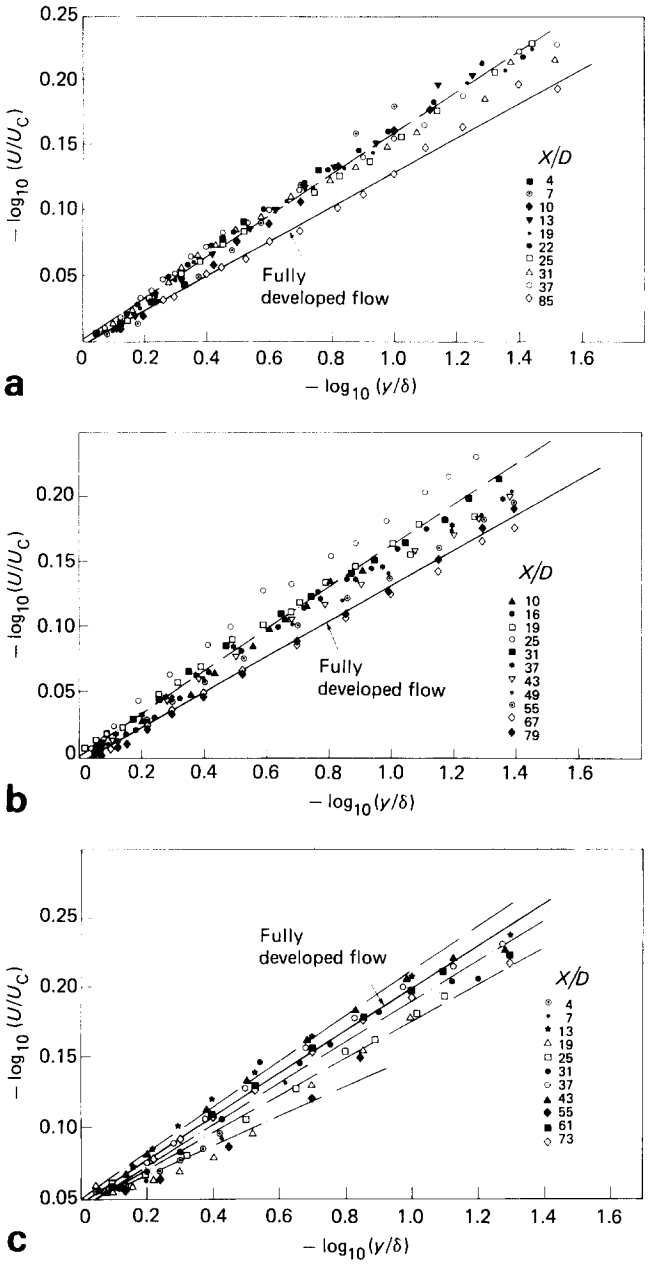

Fig 3 Data on velocity traverses in developing pipe flow plotted on a log–log basis: (a) highest flowrate; (b) medium flowrate; (c) lowest flowrate. The reciprocal of the gradient of each line gives the value of n

considerably from a value of about 12 to about 7.2 for the highest flowrate, and was almost constant for the medium flowrate but not constant at 7 as some researchers, eg Ref 14 have assumed. All the curves show a rise in the value of n as the flow becomes fully developed thus showing that there is some redistribution of flow after the boundary layer first reaches the pipe axis for all the flowrates considered.

A plot of the variation of n with x/D using two different methods is shown in Fig 5. One method is that explained for Fig 4, and the other uses data from Fig 3. The agreement between the two methods is fair for the medium flow but not quite so fair for the highest flowrate. The reason for this discrepancy is not clear. It is, however, thought to be caused by at least two things. One is the effect of turbulence on the pitot tube, which will increase with Reynolds number, and the other the effect of the presence of the tube in the thin boundary layer. As these effects are much less severe in the method using the continuity equation, the variation of n given by this method is used. It should be pointed out that this variation also gave a good correlation when used in the turbine flowmeter model[8].

The variation of n for the lowest flowrate was not considered as it would be shown later that the boundary layer was laminar.

Another plot that is now commonly used is that of the blockage factor B, defined as $1-U_0/U_c$, against x/D. This is shown in Fig 6(a) for the three flowrates considered. The curves for the medium and highest flowrate coincide at first before separating from each other. Their maxima lie between $37D$ and $45D$, which is the generally accepted value for developing turbulent flow. The curve for the lowest flow follows a different path and its maximum point occurs at around $55D$.

Fig 6(b) shows a comparison of the test results obtained for the highest flowrate when compared with Refs 1, 3 and 19. It is interesting to note that there is complete agreement with Ref 19, for which the investigation was carried out at roughly the same Reynolds number. Unfortunately, the contraction ratio used in that investigation was not given and it was therefore not possible to confirm whether the main cause of the difference in results from works on developing pipe flows could be due to this parameter. The curves for Refs 1 and 3, which were roughly at the same Reynolds number of 4×10^5, show that the results differ from one another. Although all the four curves coincided at low values of x/D, the latter two curves separated from those obtained here and their maximum points were consistently lower.

Model for developing pipe flow

Before developing a mathematical model a brief explanation of the various modes of flow in a developing flow will be given. From the plot of C_f against Re_x in Ref 20 it is seen that there is a distinct transition region for the medium and highest flowrates. There is no such transition for the lowest flowrate. The transition in the medium and highest flowrates occurred so close to the start of the test

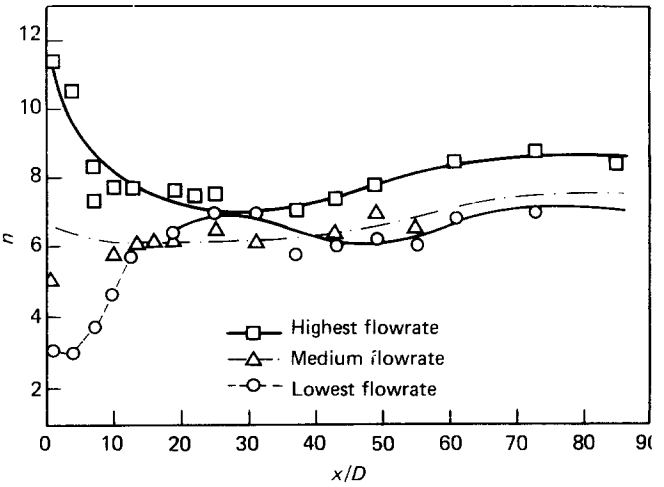

Fig 4 Variation of n *with distance from start of test pipe, using Eq (3), when* U_c/U_0 *and* δ/R *are known*

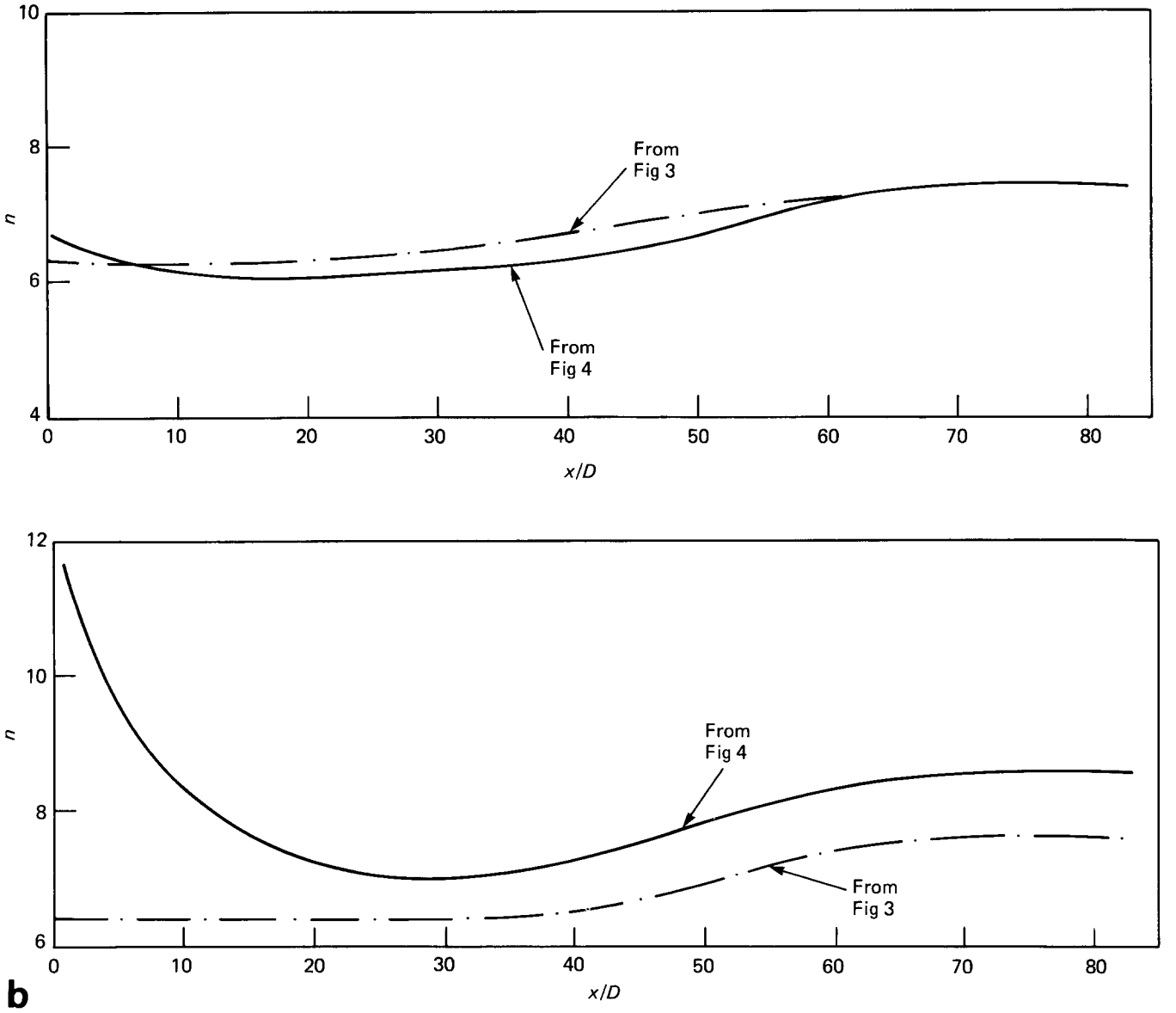

Fig 5 Comparison of variation of n *obtained from Fig 3 and that obtained from Fig 4: (a) for the medium flowrate; (b) for the highest flowrate*

length that it is assumed for all practical purposes that the turbulent boundary layer commences from this point. Most of the graphs confirm this assumption to be fair as they passed through the origin.

Fig 7(a) shows a plot of the pressure drop against distance x/D. The curves for the medium and highest flows coincide but that for the lowest flowrate is different. Also from the velocity power law curves shown in Fig 3 and the variation of B in Fig 6(a) it is clear that the flow regime for the lowest flowrate, though stable, is quite different from those of the medium and highest flowrates. It can thus be concluded that the boundary layer flow is laminar for the lowest flowrate but becomes turbulent immediately the layer reaches the pipe axis. If the boundary layer had remained laminar after it had reached the pipe centre it would perhaps have been possible to compare the results with those of Ref 15. The value of $x/R\ Re$ obtained here for the boundary layer thickness to equal the pipe radius is 0.002345 instead of the value of 0.0036 quoted in Ref 15.

Fig 7(b) is a plot of the pressure drop which is limited to where there is a central core of uniform flow. The figure shows a linear relationship between the pressure and the distance but, at some value of x/D, the curves depart from linearity. The value of x/D at which this occurs decreases with pipe Reynolds number, being smallest at the highest flowrate and not present at all for the lowest flowrate.

Another important point is that the boundary layer thickness is only about $0.62R$ when the pressure drop departs from linearity while that for the medium flow is $0.80R$. The distances from these points to the point at which the boundary layer reached the pipe axis were similar for the two flowrates. It therefore follows that the agency which is responsible for the boundary layer growth in this region is higher for the highest than for the medium flowrates. This agent is the turbulence intensity and the consequent mixing it produces. This is confirmed by the work reported in Refs 1, 2, 3 and 17, in which the centreline turbulence was measured. It is seen from that work that the turbulence intensity increases with Reynolds number. Thus, the strong mixing which starts

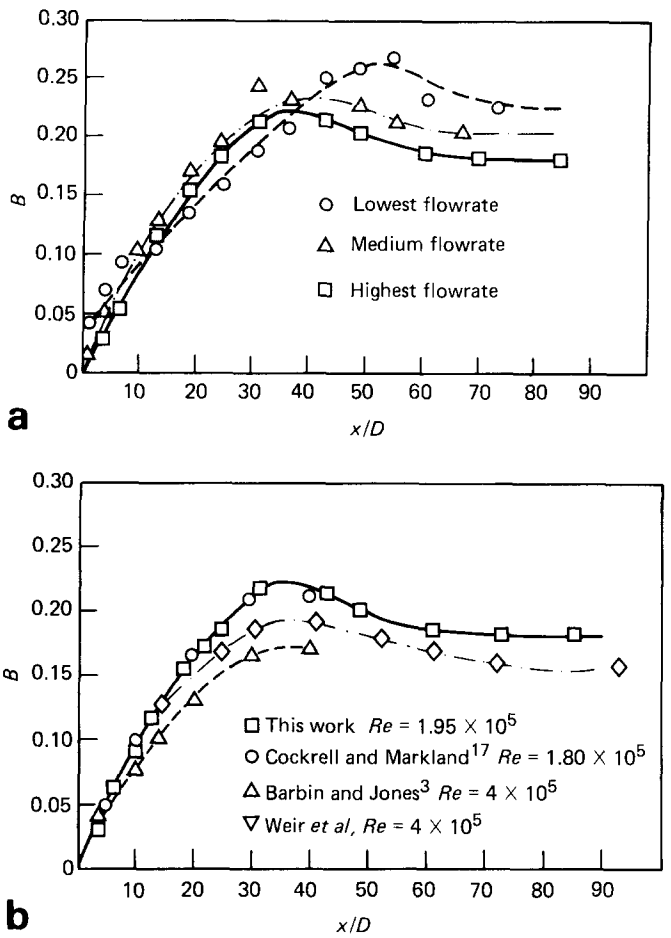

Fig 6 (a) Variation of blockage factor B *with distance from start of test pipe for the three flowrates; (b) comparison of variation of blockage factor obtained in this work and those from other sources*

to develop in the core flow now begins to sap the core of its energy. Its velocity begins to fall and eventually the core disappears completely when the layer reaches the pipe axis.

In the early portion of the developing pipe flow, where the turbulence intensity is low, the flow is not only one-dimensional but the central velocity is increasing due to the growth of the boundary layer. The flow over a flat plate is also not only one-dimensional but the turbulence intensity in the potential flow outside the layer is also small. Consequently, the flow in the pipe is like that over a flat plate with a favourable pressure gradient.

Since the centreline turbulence intensity for a fully developed pipe flow is known to be quite substantial, it is clear that this is one of the main differences between a pipe and flat plate flow. The flow now starts to depart from flat plate flow as the centreline turbulence starts to increase to that for a pipe flow. This region of rapidly increasing centreline turbulence intensity is regarded as the transition from flat plate to pipe flow. Now flat plate flow is characterized by the Reynold's number Re_x while that for the pipe is characterized by the pipe Reynolds number Re. It is therefore logical that the boundary layer growth in this region will be influenced by these two types of Reynolds number.

When the boundary layer reaches the pipe axis, the layers from opposite ends of a diameter interact with one another thus continuing the mixing process which has been noted to take place even in laminar boundary layer flow[15]. The peaky profile formed when the boundary layer thickness first equals the pipe radius, which corresponds to a low value of n in the velocity power law, becomes much flatter and the value of n increases. The end result of the mixing in this region is the production of the velocity distribution appropriate to the Reynolds number of the pipe flow. What is most important is the distance to the point at which this mixing stops, as this determines the end of the developing pipe flow.

To summarize, six flow regimes have been established in this investigation, as follows.

- *Regime 1:* laminar developing boundary layer, $x_1 - x_0$;
- *Regime 2:* transition from laminar to turbulent boundary layer, $x_2 - x_1$;
- *Regime 3:* developing turbulent boundary layer flow similar to that on a flat plate under favourable pressure gradient, $x_3 - x_2$;
- *Regime 4:* transition from flat plate flow to pipe flow, $x_4 - x_3$;
- *Regime 5:* free mixing due to interaction of boundary layers after they have reached the pipe axis, $x_5 - x_4$;
- *Regime 6:* fully developed pipe flow, $x_6 - x_5$.

In developing laminar boundary layers only regimes 1, 5 and 6 exist, although regime 5 could result in laminar pipe

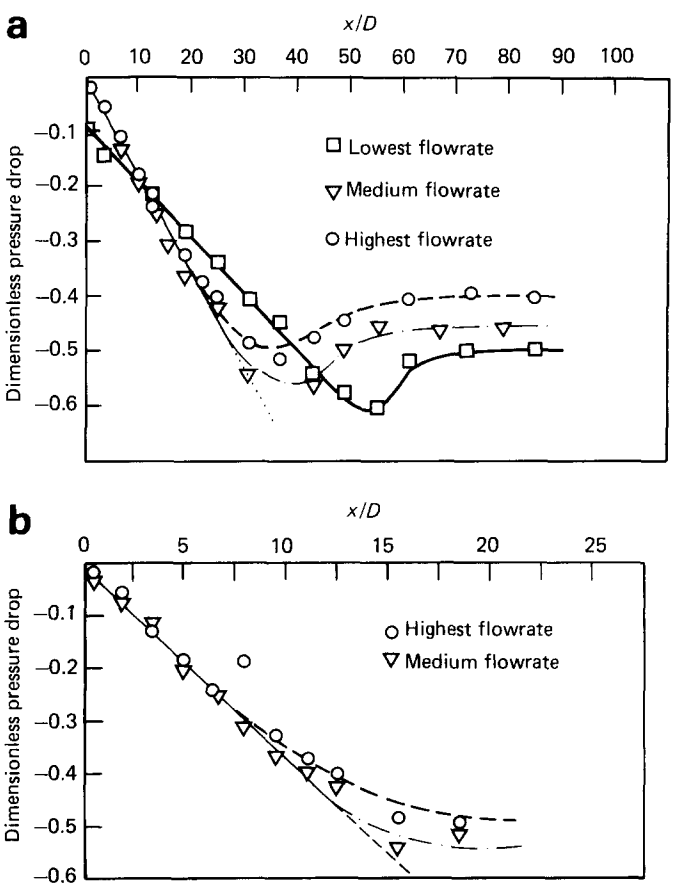

Fig 7 (a) Pressure drop, rendered dimensionless using the mean velocity, in entry portion of test pipe versus distance from start of test pipe; (b) situation for a central core of uniform flow velocity

flow as in Ref 15 or turbulent pipe flow as in the lowest flowrate used here.

Theoretical model

The model proposed is limited to the turbulent flow regimes, ie the medium and highest flowrates. It is recognized that the upstream conditions could affect the experimental results. Moreover, as the flow traversing was carried out over a period of several weeks, there could also be variation in condition of flow over the period in which the experiment was performed. Consequently, no model is being developed for the laminar and transitional regimes 1 and 2 above, which would be considerably influenced by these changes. For the two flowrates under consideration, these regimes together are very short and their effect can therefore be neglected. It is assumed that the boundary layer flow becomes turbulent right from the start of the test pipe line.

From the analysis of the developing flow carried out above, it seems that the processes that govern the development of the flow at the entry to the pipe are several. Three different models are therefore evolved to correlate the results of regimes 3, 4 and 5.

Regime 3

From the experimental investigation above it has been demonstrated that the velocity can be represented by the power law

$$\frac{U}{U_c}=\left(\frac{y}{\delta}\right)^{1/n} \tag{1}$$

while for the flow after the boundary layer has reached the pipe axis, the corresponding law is

$$\frac{U}{U_c}=\left(\frac{y}{R}\right)^{1/n} \tag{2}$$

U_c in Eq (1) is the velocity of the central core, while for the second equation it is the velocity at the pipe axis; R is the pipe radius.

It can be shown that the ratio of the mean flow to the core velocity of the developing flow is given by

$$\frac{U_0}{U_c}=\left(1-\frac{\delta}{R}\right)^2+2\left\{\frac{n}{n+1}\frac{\delta}{R}-\frac{n}{2n+1}\left(\frac{\delta}{R}\right)^2\right\} \tag{3}$$

For axisymmetric flow the displacement thickness is defined by

$$\delta^*=\int_0^R\left(1-\frac{U}{U_c}\right)\left(1-\frac{y}{R}\right)\mathrm{d}y \tag{4}$$

and the momentum thickness by

$$\theta=\int_0^R\left(1-\frac{U}{U_c}\right)\frac{U}{U_c}\left(1-\frac{y}{R}\right)\mathrm{d}y \tag{5}$$

By inserting Eq (1) into Eqs (4) and (5) it can be shown that

$$\frac{\delta^*}{R}=\frac{1}{n+1}\frac{\delta}{R}-\frac{1}{2(2n+1)}\frac{\delta^2}{R^2} \tag{6}$$

while

$$\frac{\theta}{R}=\frac{n}{(n+1)(n+2)}\frac{\delta}{R}-\frac{n}{(2n+1)(2n+2)}\frac{\delta^2}{R^2} \tag{7}$$

Now the integral momentum equation is given by

$$\frac{\mathrm{d}\theta}{\mathrm{d}x}+\frac{2\theta+\delta^*}{U_c}\frac{\mathrm{d}U_c}{\mathrm{d}x}=\frac{C_f}{2} \tag{8}$$

where C_f is the local coefficient of friction. By differentiating Eq (3) it can be shown that

$$\frac{U_0}{U_c}\frac{\mathrm{d}U_c}{\mathrm{d}x}=\left(\frac{2}{n+1}\frac{1}{R}-\frac{2}{2n+1}\frac{\delta}{R^2}\right)\frac{\mathrm{d}\delta}{\mathrm{d}x} \tag{9}$$

Also

$$\frac{2\theta+\delta^*}{F}=\frac{3n+2}{(n+1)(n+2)}\frac{\delta}{R}-\frac{3n+1}{(2n+1)(2n+2)}\frac{\delta^2}{R^2} \tag{10}$$

$$\therefore\quad \frac{2\theta+\delta^*}{U_c}\frac{\mathrm{d}U_c}{\mathrm{d}x}=$$

$$\left\{\frac{\left(\frac{2}{n+1}-\frac{2}{2n+1}\frac{\delta}{R}\right)\left(\frac{3n+2}{(n+1)(n+2)}\frac{\delta}{R}-\frac{3n+1}{(2n+1)(2n+2)}\frac{\delta^2}{R^2}\right)}{\left(1-\frac{\delta}{R}\right)^2+2\left(\frac{n}{n+1}\frac{\delta}{R}-\frac{n}{2n+1}\frac{\delta^2}{R^2}\right)}\right\}\frac{\mathrm{d}\delta}{\mathrm{d}x} \tag{11}$$

and

$$\frac{\mathrm{d}\theta}{\mathrm{d}x}=\left\{\frac{n}{(n+1)(n+2)}-\frac{2n}{(2n+1)(2n+2)}\frac{\delta}{R}\right\}\frac{\mathrm{d}\delta}{\mathrm{d}x} \tag{12}$$

The coefficient of friction for a flat plate is[21]

$$\frac{C_f}{2}=\frac{0.02888}{\left(\log 4.075\frac{U_c\theta}{\nu}\right)^2}=\left(3.595+5.893\log\frac{U_c\theta}{\nu}\right)^{-2}$$

$$=\left\{3.595+5.893\log\frac{U_0 d}{\nu}+5.893\log\frac{\theta}{2R}\frac{U_c}{U_0}\right\}^{-2}$$

$$=\left[3.294+5.893\log\frac{U_0 d}{\nu}\right.$$

$$\left.+5.893\log\left\{\frac{\frac{n}{(n+1)(n+2)}\frac{\delta}{R}-\frac{n}{(2n+1)(2n+2)}\frac{\delta^2}{R^2}}{\left(1-\frac{\delta}{R}\right)^2+2\left(\frac{n}{n+1}\frac{\delta}{R}-\frac{n}{2n+1}\frac{\delta^2}{R^2}\right)}\right\}\right]^{-2} \tag{13}$$

Inserting Eqs (11), (12) and (13) into Eq (8) and integrating gives

$$\frac{x-x_2}{R}=\int_0^1\left[\left\{\frac{n}{(n+1)(n+2)}-\frac{2n}{(2n+1)(2n+2)}\frac{\delta}{R}\right\}+\right.$$

$$\left.\frac{\left\{\frac{2}{(n+1)}-\frac{2}{(2n+1)}\frac{\delta}{R}\right\}\left\{\frac{3n+2}{(n+1)(n+2)}\frac{\delta}{R}-\frac{3n+1}{(2n+1)(2n+2)}\frac{\delta^2}{R^2}\right\}}{\left(1-\frac{\delta}{R}\right)^2+\frac{2n}{(n+1)}\frac{\delta}{R}-\frac{2n}{(2n+1)}\frac{\delta^2}{R^2}}\right]$$

$$\times\left[3.294+5.893\log\frac{U_0 d}{\nu}\right.$$

$$\left.+5.893\log\left\{\frac{\frac{n}{(n+1)(n+2)}\frac{\delta}{R}-\frac{n}{(2n+1)(2n+2)}\frac{\delta^2}{R^2}}{\left(1-\frac{\delta}{R}\right)^2+\frac{2n}{(n+1)}\frac{\delta}{R}-\frac{2n}{(2n+1)}\frac{\delta^2}{R^2}}\right\}^2\right]\frac{\mathrm{d}\delta}{R} \tag{14}$$

The above formula can be plotted as a function of $dx/R = f(\delta)\,d\delta/R$ and then solved by graphical integration to obtain $x - x_2/R$.

Regime 4

For this regime it was noted from the above that the boundary layer growth increases with the turbulence intensity, which is characterized by the pipe Reynolds number, and the history of the flow, which is characterized by the length from the start of the mixing process. Thus, mathematically,

$$\frac{\delta-\delta_3}{R} = f\left(Re, \frac{x-x_3}{R}\right) \tag{15}$$

where subscript 3 refers to the end of regime 3. By careful examination of the experimental results in this region it is found that a suitable relation is

$$\frac{\delta-\delta_3}{R} = A\left(\frac{x-x_3}{R}\right)^{1/2} Re$$

$$\therefore \quad \frac{\Delta\delta}{R} = A\left(\frac{\Delta x}{R}\right)^{1/2} Re \tag{16}$$

where $\Delta\delta = \delta - \delta_3$ and $\Delta x = x - x_3$.

Regime 5

In this regime the value of n dropped linearly with distance along the pipe. It was this that lead to the correlation of the form

$$n = f(Re_x) \tag{17}$$

Discussion

The early part of Fig 8 shows the development of the boundary layer obtained from Eq (14) for both medium and highest flowrates using values of n from Fig 4. Because the agreement with the experimental results in this regime is fair it could be concluded that the flow at the entry to the pipe is similar to developing flow on a flat plate with a favourable pressure gradient.

For the region where the central core becomes highly turbulent, regime 4, a curve of $(\Delta x/R)^{1/2}$ plotted against $(\Delta\delta/R)(1/Re)$ is drawn as shown in Fig 9. The figure shows that there is a linear relationship. Thus

$$\left(\frac{\Delta x}{R}\right)^{1/2} = 3.6\times10^5 \frac{\Delta\delta}{R}\left(\frac{1}{Re}\right) \tag{18}$$

for the flowrates. With this equation it was possible to complete the development of the boundary layer up to the pipe axis as shown in Fig 8. The full lines are the theoretical models obtained from Eqs (14) and (18). The overall agreement looks fair.

Another interesting point was that the start of regime 4 is roughly at the same value of Reynolds number Re_x and this was found to be about 3.1×10^6 and 3.2×10^6 for the highest and medium flowrates, respectively. From Refs 1 and 3 the corresponding figures were about 4.3×10^6 and 3.9×10^6, respectively. Because of the scale

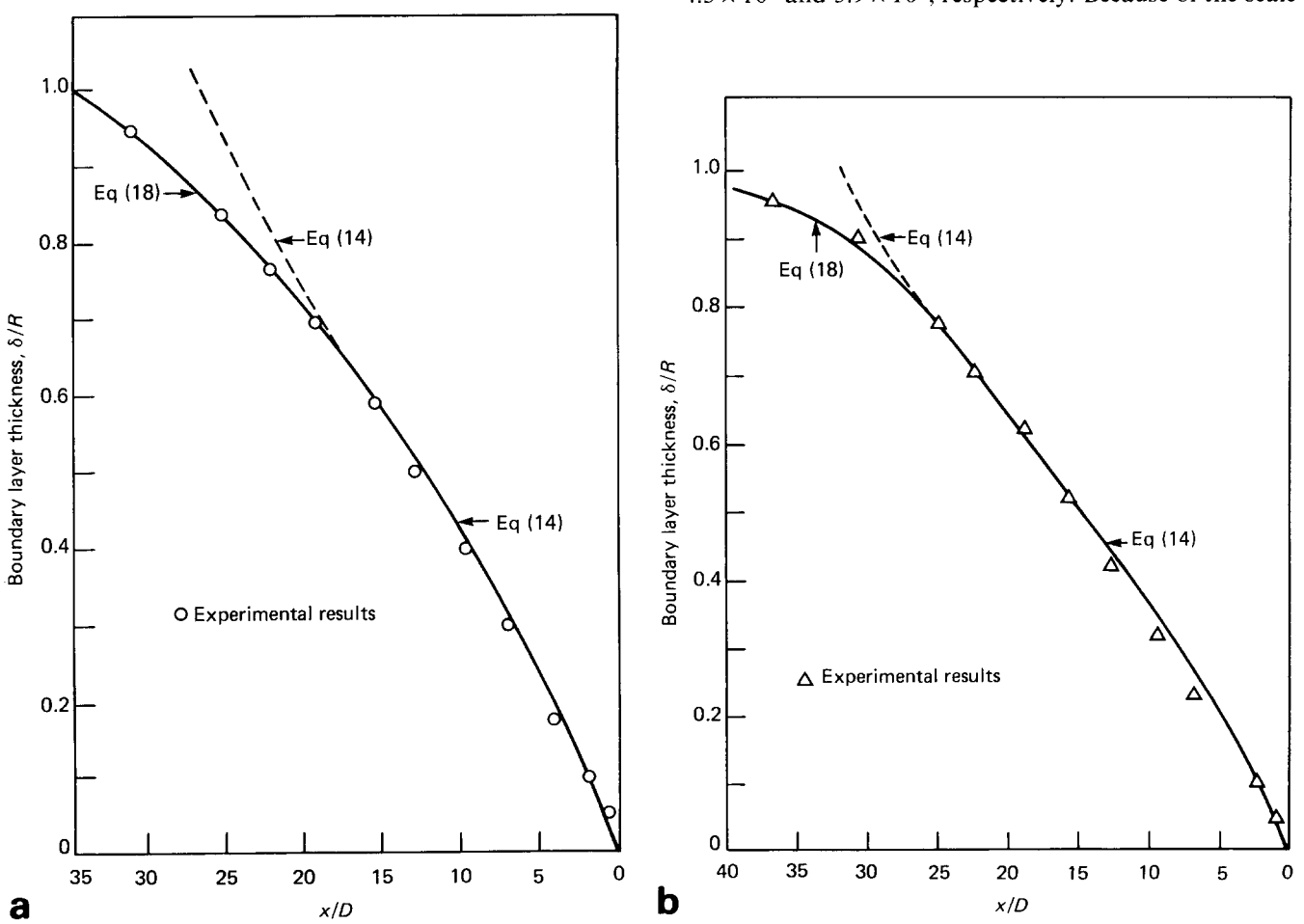

Fig 8 Prediction of development of boundary layer in regimes 3 and 4: (a) highest flowrate; (b) medium flowrate

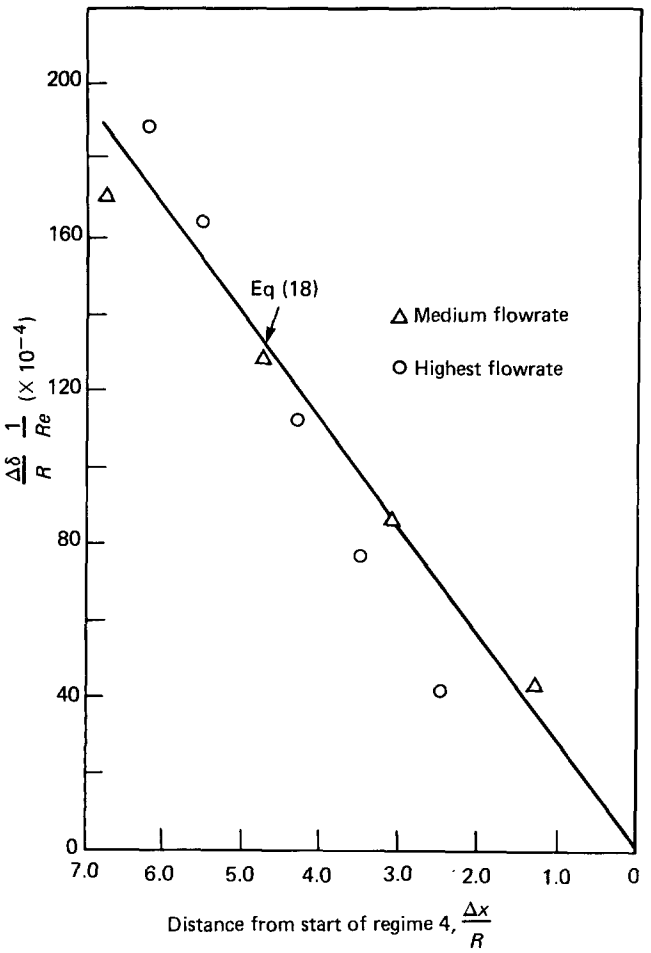

Fig 9 Development of boundary layer with distance in regime 4

of the diagrams it was not possible to read these points very accurately. Results from Ref 2 showed that the regime started at the beginning of the test pipe line.

In regime 4 as the turbulence started increasing, the velocity at the core began to decrease. This was, however, not manifested in the lowest flowrate, where the velocity at the pipe axis continued to increase until the boundary layer eventually reached the pipe axis. Fig 4 shows that in the regions just before the boundary layers reached the pipe axis, the values of n are similar for the three flowrates. When a plot is made of the boundary layer momentum thickness θ against distance, Fig 10(a) is obtained, from which it is seen that the relationship is linear at first but later begins to depart from linearity. If, however, the central velocity is taken to be what it would have been for the two higher flowrates, ie if regime 4 had never existed, a unique graph is obtained (Fig 10(b)).

Fig 9 shows some scatter. This is attributed to the fact that the experiment took place over a period of a few months during which time the fluid properties, level of turbulence, etc, may have changed slightly. As the regime coincides with the part of the flow which is highly turbulent, it is possible that the boundary layer growth could be influenced by changes in the upstream conditions of the flow.

In regime 5 for all the flowrates there is a decrease in the value of n. A plot of n against Re_x shows a linear relationship which was unique for this region. Fig 11 shows the relationship, n here being the value for the fully developed flow, and is given by

$$n = 5.16 + 2.8 \times 10^{-6}\, Re_x \qquad (19)$$

Nikuradse has done a great deal of work relating the value of n to the pipe Reynolds number. However, from

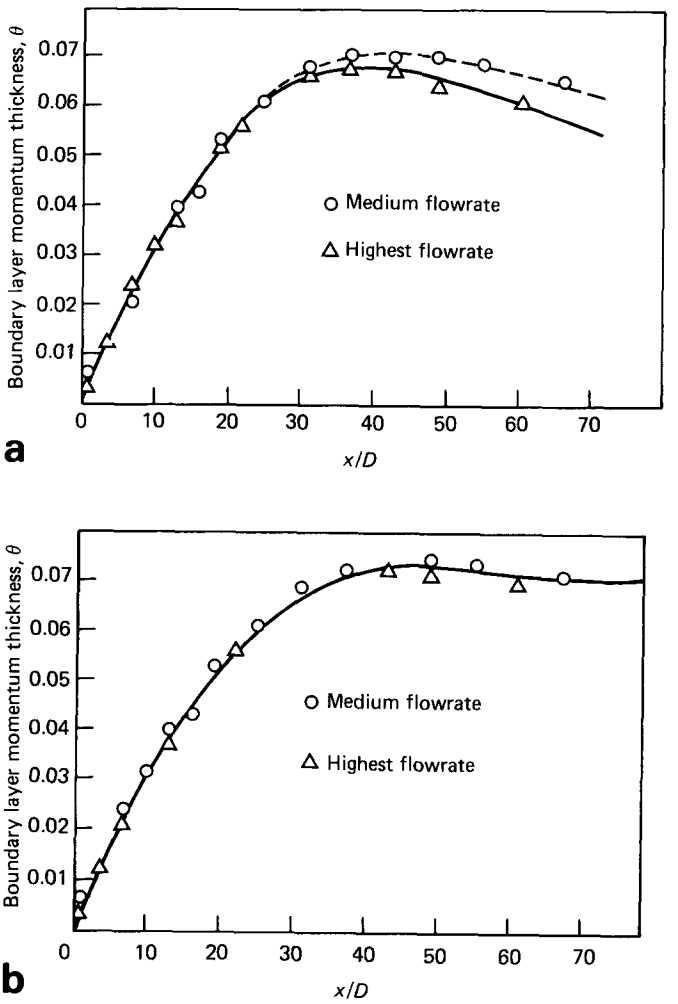

Fig 10 Development of boundary layer momentum thickness: (a) based on actual core velocities; (b) based on the assumption of low intensity of turbulence of the central core

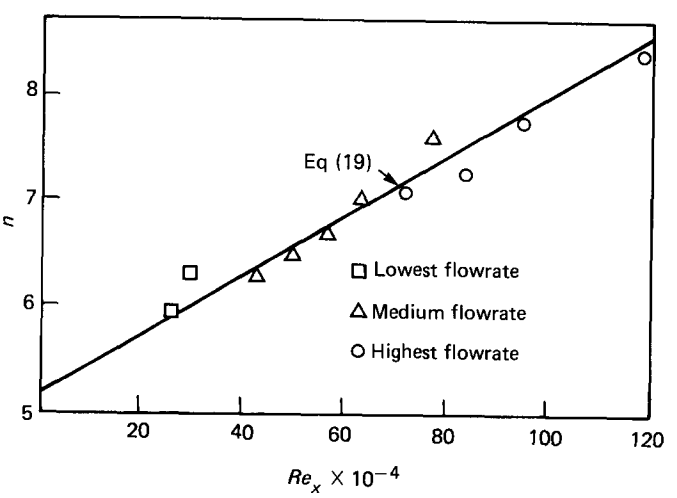

Fig 11 Variation of n *with Reynolds number* Re_x *in regime 6*

recent studies and also the present investigations of a developing boundary layer, it appears that Nikuradse may have been traversing the flow in the mixing region of regime 5. It is therefore possible that the actual value of n could be slightly higher than that obtained by him, as has been obtained here.

The above correlation would be quite useful in determining when a flow is truly fully developed. From the Reynolds number Re of the flow it would be possible to obtain n, while Fig 11 would give the value of Re_x. The length of pipe required for the flow to be fully developed would be given by x/D, which is also the ratio of Re_x/Re.

Another deduction that could be made from the present investigation is that it appears that the degree of uniform flow emerging from a contraction not only depends on the contraction ratio but also on the velocity of flow. Consequently, the higher the velocity the flatter the profile. It appears the flattening of the profile could have been due to the thinning down of the initial boundary layer from the larger pipe by the reducing piece. If the flowrate is small the boundary layer persists even though it is considerably reduced (see Fig 2) but if the flow is large, it almost completely disappears and the velocity profile is flat. The boundary layer also changes to laminar in the process.

From the plot of blockage factor B against distance (Fig 6(a)) it is noted that the curves separate from the linear portion of the graph, starting with the highest Reynolds number. It is not clear whether the distance at which the departure starts will continue to fall indefinitely with Reynolds number, although the work of Miller[2] carried out at $Re = 5.5 \times 10^5$ seems to suggest this. If this is the case, regime 3 will disappear completely, or become so small that its influence becomes negligible at very high Reynolds numbers. On the other hand, decreasing the Reynolds number will delay the departure and hence the onset of regime 4. It is therefore possible that at sufficiently low Reynolds number, regime 4 may not exist, even though the boundary layer is turbulent.

The above may therefore explain the variation of n with distance. At high Reynolds number the velocity comes out with a much flatter profile, ie higher n, but this gradually reduces to a lower value of around 7 as the boundary layer develops. For the medium flow the profile is not as flat; thus, the value of n is lower than that for the highest flowrate and remains almost constant throughout up to the end of regime 4. At the pipe entry for the lowest flowrate the velocity is not flat, and the value of n falls. The comparison cannot continue beyond this point because the flow is laminar.

Conclusion

In the investigation described above, the various flow regimes that can exist in the developing flow in the entry region of a circular pipe have been discussed. For a turbulent developing boundary layer there are six regimes, while for laminar flow there are only three. There could be cases where laminar developing flow becomes turbulent, when the boundary layer reaches the pipe axis, as shown by the lowest flowrate.

Based on the above, and limiting the work to turbulent developing flows, mathematical models were evolved for three flow regimes, referred to as regimes 3, 4 and 5, which coincided with flat plate flow under a favourable pressure gradient, transition from plate to pipe flow, and after the boundary layer has reached the pipe, respectively. The models for regimes 3 and 4 enabled the growth of the boundary layer to be predicted up to the time it reached the pipe axis. The agreement with experimental data was quite satisfactory. The model for regime 5 was found to be quite useful in determining when the boundary layer was fully developed. It may be necessary to find a fresh relationship between the reciprocal exponent n of the velocity power law and the pipe Reynolds number now that it is becoming clear that the region at which Nikuradse traversed the flow may not have been the fully developed flow regime.

The onset of the transition from flat plate to pipe flow, which coincided with increase in the centreline turbulence, took place at roughly the same value of Reynolds number Re_x, of about 3.15×10^6. Corresponding figures from other researchers were between 3.9×10^6 and 4.3×10^6.

References

1. **Weir J., Priest A. J. and Sharan V. K.** Research note on the inlet disturbances in turbulent pipe flow. *J. Mech. Eng. Sci., 1974*, **16**(3), *211–213*
2. **Miller, D.** Performance of straight diffuser, part II: internal flow. *A Guide to Losses in Pipes and Duct Systems, BHRA Fluid Engineering, Cranfield, 1971*
3. **Barbin A. R. and Jones J. B.** Turbulent flow in the inlet Region of a smooth pipe. *ASME Trans. J. Basic Eng., 1963*, **85**(*1*), *29–34*
4. **Patel R. P.** A note on fully developed flow down a circular pipe. *Aeronaturical J. 1974*, **78**(*2/3*), *93–97*
5. **Klein A.** Review of turbulent developing pipe flow. *ASME J. Fluid Eng., June 1981*, **102**(*2*), *243–249*
6. **Wang, Jeng-Song and Tullis J. P.** Turbulent flow in the entry region of a rough pipe. *ASME J. Fluid Eng., 1974*, **96**(*1*), *62–68*
7. **Jepson P. and Bean P. G.** Effects of upstream velocity profiles on turbine flowmeter registration. *J. Mech. Eng. Sci. Oct 1969*, **11**(*5*)
8. **Salami L. A.** Effect of Velocity Profile just Upstream of a Turbine Flowmeter on its Characteristics, *Univ. of Southampton Report MEE/72/2, Jan 1972*
9. **Fillipov G. V.** On turbulent flow in entrance length of a straight tube of circular cross-section. *Soviet Phys. - Tech. Phys. 1958*, **32**(*8*), *1681–1686*
10. **Ross D. and Whippany N. J.** Turbulent flow in the entrance region of a pipe. *Trans. ASME J. Series D, Dec 1956*, **78**(*4*), *915–923*
11. **Holdhusen J. S.** Turbulent Boundary Layer in the Inlet Region of Smooth Pipes, *PhD Dissertation, Univ. of Minnesota, 1952*
12. **Diessler R. G.** Turbulent heat transfer and friction in the entrance region of smooth passages. *Trans. ASME, 1955*, **77**, *1221–1233*
13. **Latzco H.** Heat transmission to a turbulent flow of liquid or gas. *Abhandlungen aus dem Aerodynamischen Institut und der Technishen Hochshule, Aachen, Vol 1, 1921;* also *NACA 1068, 1944*
14. **Bowles A. and Brighton J. A.** Incompressible turbulent flow in the inlet region of a pipe. *J. Basic Eng., Trans. ASME Series 3, 1968*, **90**(*3*), *431–433*
15. **Mohanty A. K. and Asthana S. B. L.** Laminar flow in the entrance region of a smooth pipe. *J. Fluid Mech. Feb 1979*, **90**(*3*), *433–447*
16. **Sale D. E.** Entrance Effect of Incompressible Diffuser Flow, *MSc Thesis, University of Manchester, 1967*
17. **Ower E. and Pankhurst R. C.** *The Measurement of Air Flow, Pergamon Press, Oxford, 4th Edn 1969, 48*
18. **Salami L. A.** Effects of Turbine Flowmeter and the Effectiveness of Different Types of Flow Straightener, *Univ. of Southampton Report MEE/72/3, Jan 1972*

19. **Cockrel D. J. and Markland E.** The effect of inlet conditions on incompressible flow through conical diffuser. *J. Royal Aeronautical Soc., 1962*, **66**(*1*), *51–52*

20. **Salami L. A.** Towards standardization of turbine-type flowmeters. *Proc. Int. Conf. on Advances in Flow Measurement Technique, BHRA Fluid Engineering, Sept 1981, 279–292*

21. **Squire H. B. and Young A. D.** *The Calculation of Profile Drag on Airfoils Aeronautical Research Council R&M, 1938*